

Electron dynamics in vacancy islands

H. Jensen, J. Kröger,* and R. Berndt

*Institut für Experimentelle und Angewandte Physik,
Christian-Albrechts-Universität zu Kiel, D-24098 Kiel, Germany*

S. Crampin[†]

Department of Physics, University of Bath, Bath BA2 7AY, United Kingdom

The dynamics of Ag(111) surface state electrons confined to nanoscale hexagonal and triangular vacancy islands are investigated using scanning tunneling spectroscopy. The lifetimes of quantised states with significant amplitude near the centers of the vacancies are weakly affected by the geometry of the confining cavity. A model that includes the dependence of the lifetime on electron energy, vacancy size, step reflectivity and the phase coherence length describes the results well. For vacancy islands with areas in the range $\approx 40\text{--}220\text{ nm}^2$ lossy scattering is the dominant lifetime-limiting process. This result and a corrected analysis of published experimental data improve the consistency of experimental and calculated surface state lifetimes.

PACS numbers: 73.20.At, 72.10.Fk

Spectacular real-space observations of electron confinement have been realized by scanning tunneling microscopy (STM) and scanning tunneling spectroscopy (STS) for the Shockley-type electronic surface states on the (111) surfaces of the noble metals. Electron confinement to artificial (*e.g.*, Refs. 1,2,3,4,5) and natural (*e.g.*, Refs. 6,7,8,9) nanostructures has been studied in some detail. Moreover, several reports have addressed the lifetime of surface state electrons as deduced from tunnelling spectroscopy of large terraces, scattering patterns near steps and in confining structures.^{5,6,10,11,12} Currently, however, the influence of the confinement on electronic lifetimes is not clear.

Using low-temperature STS of triangular and hexagonal vacancy islands and model calculations, we investigate the effects of the geometry of the confining resonator and of lossy scattering at its boundary on the lifetimes of confined states. For the states investigated, which have an antinode at the center of these resonators, we find similar lifetimes independent of the geometry. Lossy scattering at the confining step edges turns out to be the lifetime-limiting process.

The experiments were performed in ultrahigh vacuum (base pressure 1×10^{-8} Pa) at 9 K using a custom-made microscope. Tungsten tips and Ag(111) were prepared by argon ion bombardment and annealing. Hexagonal vacancy islands were fabricated by briefly (2–3 s) exposing freshly prepared Ag(111) surfaces to a low-flux argon ion beam.¹³ The resulting nanostructures are shown in Fig. 1. Triangular vacancy islands were obtained through controlled tip-sample contacts. The differential conductivity (dI/dV) was measured by superimposing a sinusoidal voltage modulation (3 mV_{rms}, 10 kHz) on the tunneling voltage and measuring the current response by a lock-in amplifier.

Maps of dI/dV from a hexagonal vacancy island (Fig. 2a) exhibit strongly voltage-dependent features, similar to those found from, *e.g.* hexagonal Ag islands.^{6,8} For voltages below the Ag(111) surface state band edge at

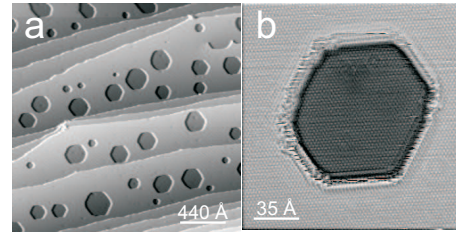


FIG. 1: (a) Topographic image of Ag(111) surface after low-flux Ar^+ bombardment. (b) Atomically resolved vacancy island which serves as the cavity for electron confinement.

$E_0 \approx -67$ mV the interior of the vacancy island is featureless while at higher voltages increasing numbers of sixfold azimuthally symmetric rings occur. The sixfold modulation is partially distorted due to deviations of the vacancy island from a perfect hexagonal shape. dI/dV being related to the local density of states,¹⁴ the interference patterns are attributed to surface state standing waves confined by scattering at the edges of the island. Figure 2b shows similar data for a triangular vacancy island. Starting from a featureless interference pattern at -60 mV, increasingly complex patterns occur at higher voltages. The number of antinodes increases with higher voltages as expected from a particle-in-a-box model. At -20 mV, for instance, six antinodes of the local density of states are clearly visible.

For a quantitative measure of the confinement we acquired dI/dV spectra above the vacancy island centers. A typical spectrum of a hexagonal island (Fig. 3a) is comprised of a series of peaks with the first appearing just above the lower band edge of the Ag(111) surface state. The peak width increases with increasing energy. These peaks correspond to the energy levels of the confined Ag(111) surface state electrons, with the broadening into resonances as a result of single-particle scattering processes,^{2,15} many-body interactions,¹⁶ and instrumen-

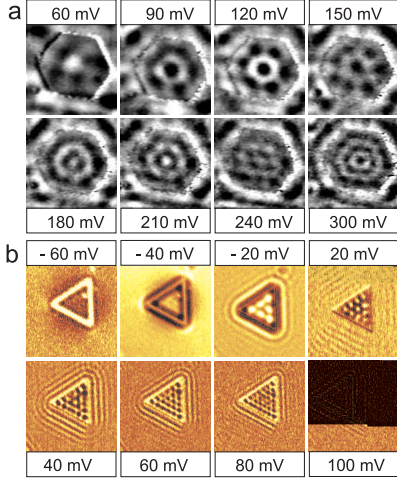


FIG. 2: (a) Series of constant-current dI/dV maps of a hexagonal vacancy island with edge length ≈ 5.8 nm recorded at indicated sample voltages (white corresponds to large dI/dV). (b) Analogous data for a triangular vacancy with edge length 22 nm.

tal effects such as the finite modulation voltage and finite temperature. We have confirmed this interpretation using the same approach as in Refs. 6,8 using a variational embedding technique¹⁷ to compute the electronic structure of two-dimensional electrons with effective mass m^* confined to hexagonal or triangular domains by an infinite barrier. This gives a series of discrete levels at energies that are dependent upon the size and geometry of the confined region, which we broaden by including an empirically determined self-energy $\text{Im} \Sigma \approx 0.2(E - E_F)$, where E_F is the Fermi energy. Note that in comparing the experimental data with calculated spectra the true dimensions of the island must be determined. It is not *a priori* clear that the relevant dimension of the island coincides with its apparent topographic boundaries, for example due to the finite spatial extension of the tip the topographic dimensions are expected to be smaller than the actual ones. Consequently, we fit the experimental dI/dV curves by calculated spectra varying the edge length as the only fit parameter. The full line in Fig. 3a depicts the result of this fit procedure applied to the vacancy island with a topographic edge length of 7.4 nm. The fit parameter, however, is given by 7.6 nm. Performing this fit procedure for several island sizes we find that the topographs of the vacancy islands tend to underestimate the actual sizes.

We now discuss the lifetimes of the quantised electron states which are proportional to the inverse width of the associated peaks in the dI/dV spectra. In particular the half width at half maximum (HWHM) of the electron levels corresponds to an energy uncertainty ($\text{Im} \Sigma$) related

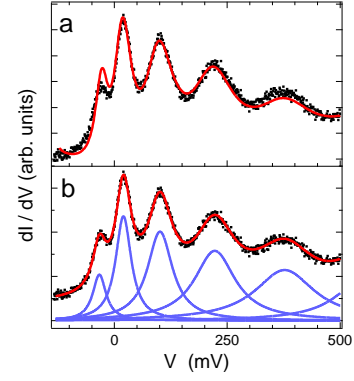


FIG. 3: (a) Experimental dI/dV data (dots) fitted by calculated spectrum (full line) based on a variation calculation as explained in the text. (b) Experimental dI/dV spectrum (dots) fitted by superposition of Lorentzians (full lines). Topographic edge length of the island is 7.4 nm.

to the lifetime τ of the electronic state via

$$\tau = \hbar / (2 \text{Im} \Sigma) \approx [329 \text{ meV fs}] / \text{Im} \Sigma. \quad (1)$$

In analysing the peak width, instrumental broadening due to voltage modulation and thermal effects have been taken into account. A fit using 5 Lorentzians plus an additional one at high energies to match the background is shown in Fig. 3b. Taking the HWHM of the Lorentzians we arrive at the corresponding imaginary parts of the self energy, which is converted to a lifetime using (1). Figure 4 displays the electronic lifetimes versus their binding energies as extracted from various hexagonal and triangular vacancy islands, along with data from several other Ag(111) surface state lifetime studies, both experimental and theoretical. While a general trend of increasing lifetime as the binding energy approaches the Fermi level is obvious, there are significant differences in magnitudes, to be discussed next.

We first note from the vacancy data of Fig. 4 that the geometric shape of the confining structure has little impact on lifetimes. Consequently, in modeling, we consider a *circular* vacancy island where the high symmetry permits a relatively simple description. In particular, one can show¹⁸ that the confined levels occur at energies for which

$$R e^{2ikS} e^{-S/L_\Phi} e^{-i\pi/2} = 1. \quad (2)$$

S is the radius of the vacancy, $k = \sqrt{2m^*(E - E_0)/\hbar^2}$ is the magnitude of the surface electron wave vector, and R is the reflection coefficient describing scattering from the confining atomic step. Eq. 2 is similar to the round trip phase condition for surface states in the phase accumulation model,^{19,20} where electrons undergoing multiple reflections at barriers with reflection coefficients R_l and R_r separated by distance d are found at energies given by $R_l R_r \exp 2ikd = 1$. In the vacancy island the round trip corresponds to starting and finishing at the center

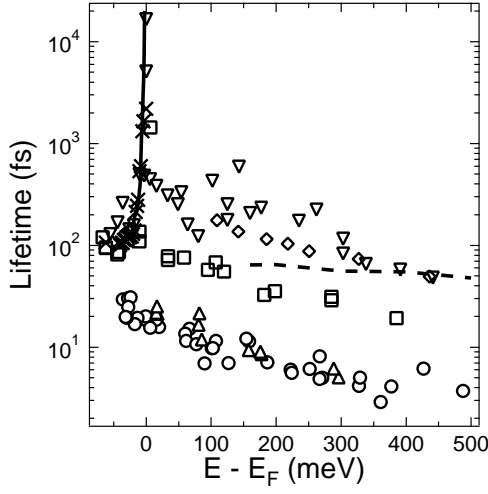


FIG. 4: Lifetime versus binding energy $E - E_F$ found for Ag(111) surface state electrons confined to vacancy hexagons (\circ), vacancy triangles (Δ), triangular corrals of Ag adatoms (∇ , adapted from Ref. 5), circular and rectangular corrals of Mn adatoms (\square , adapted from Ref. 4); lifetimes extracted from standing wave patterns near step edges (\diamond , adapted from Refs. 11,12); photoemission data (\times , from Ref. 21); results of theory are depicted as a full and a dashed line (from Refs. 21 and 12, respectively).

and only involves one reflection — so just one reflection coefficient appears in (2) — and in the vacancy island the wave function must have an antinode at the center to be visible in STS, so that the round trip phase corresponds to an odd number of half wavelengths. This is the effect of the $\exp -i\pi/2$ factor in (2). One final difference is that (2) also takes into account many-body interactions through the factor containing L_Φ , the phase relaxation length due to electron-electron (e-e) and electron-phonon (e-p) scattering. L_Φ is related by the group velocity $v_g = \hbar k/m^*$ to the corresponding inelastic scattering lifetime τ_1 : $L_\Phi = v_g \tau_1$.

Writing $R = \exp(i(\phi_R - i \ln |R|))$, Eq. 2 is satisfied when

$$\phi_R - i \ln |R| + 2kS + iS/L_\Phi - \pi/2 = 2\pi n \quad (3)$$

for $n = 1, 2, \dots$, which has solutions at complex energies $E - i \text{Im} \Sigma$. Assuming $\text{Im} \Sigma \ll (E - E_0)$, the real and imaginary parts of Eq. 3 give the energy of the n 'th level

$$E_n = E_0 + \frac{\hbar^2(n\pi + \pi/4 - \phi_R/2)^2}{2m^* S^2} \quad (4)$$

and corresponding width

$$\text{Im} \Sigma_n = \frac{\hbar v_g}{2} \left[-\frac{\ln |R|}{S} + \frac{1}{L_\Phi} \right] \quad (5)$$

where v_g , $|R|$ and L_Φ are evaluated at the energy E_n . Hence the lifetime of the surface state electrons confined

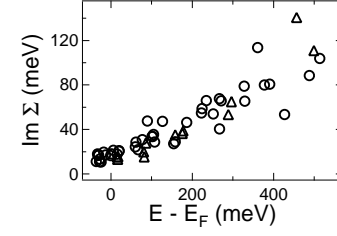


FIG. 5: Hexagon (\circ) and triangle (Δ) data from Fig. 4, represented as $\text{Im} \Sigma$ versus binding energy $E - E_F$.

within the vacancy islands is given by

$$\tau^{-1} = \tau_R^{-1} + \tau_1^{-1} \quad (6)$$

where the lifetime τ_R associated with lossy scattering at the atomic step is

$$\tau_R = -\frac{S}{v_g \ln |R|}. \quad (7)$$

At 225 meV, Echenique and co-workers¹² find $\tau_1 \approx 62$ fs in calculations that include the surface band structure, and which treat e-e interactions within the GW approximation¹⁰ and use the full Eliashberg spectral function for the e-p interaction.²¹ Bürgi *et al.*⁷ have measured the reflection coefficient for surface state scattering at ascending steps on Ag(111) and report $|R| \approx 0.23 \pm 0.07$ at 225 meV. Using Eq. 7 (and $m^* = 0.4 m_e$)¹¹ this gives $\tau_R \approx (9 \pm 2)$ fs for an island with edge 7.5 nm, and from (6) a lifetime of $\tau \approx (7.9 \pm 1.5)$ fs. This is consistent with our measured lifetimes shown in Fig. 4. The calculated result is exemplary for the overall consistency with our measured lifetime data. We can therefore conclude that at this energy the electron states within the vacancy island are roughly 8 times more likely to decay via lossy scattering at the confining boundary than via inelastic e-e and e-p scattering. Repeating this analysis at other energies, we find that the lossy boundary scattering is the dominant lifetime-limiting process for all islands that we have studied. They would need to be typically an order of magnitude larger in dimension for the inelastic e-e and e-p scattering to become dominant.

Bürgi *et al.*⁷ find that $|R|$ decreases with increasing energy. Using their values we find that $-\ln |R|$ varies approximately as $(E - E_0)^{1/2}$. Since $v_g \propto (E - E_0)^{1/2}$ and since L_Φ^{-1} is negligible with respect to $\ln |R|/S$ in Eq. 5 due to the dominance of the lossy-scattering mechanism the level width increases approximately linearly with energy. Figure 5 shows our results for the linewidths as a function of energy, which demonstrate this behavior. A similar variation in level width was previously inferred by Li *et al.*⁶ for surface state confinement to adatom islands, where a phenomenological self energy $\text{Im} \Sigma = 0.2 (E - E_0)$ was found to match the observed level broadening. Bürgi *et al.*⁷ have shown that the reflection coefficient for descending steps, which surround adatom islands, varies in a similar manner to that for ascending steps.

In Fig. 4 various other lifetime data are shown. The Mn corral values obtained by Kliewer *et al.*⁴ (\square) have been obtained by analysing experimentally determined spectral linewidths using the two-dimensional “black-dot” scattering model introduced by Heller and coworkers.² The lifetime is obtained using Eq. 1 where $\text{Im}\Sigma$ is the electron self energy needed to bring calculated spectra into agreement with measured ones. In effect, the lifetime is assumed to be due to e-e/e-p scattering, and hence to be identified as τ_1 , as the scattering properties of the confining adatom array is incorporated via the multiple-scattering equations. However, the nature of the system is similar to the present one, with the total linewidth a sum of contributions due to lossy scattering and the e-e/e-p scattering. Hence the assumption that Mn adatoms act as “black-dot” scatterers means that the lifetime values that have been obtained should be viewed as lower limits to τ_1 . The true reflectivity of the Mn adatom corrals is likely to be lower than that of the assumed “black-dot” scatterers, meaning that the lossy scattering is actually greater than modelled. Hence a smaller amount of the measured linewidth should be attributed to e-e/e-p scattering, increasing τ_1 .

The lifetimes deduced from the decay of standing wave patterns^{11,12} at steps shown in Fig. 4 (\diamond) are not complicated by lossy scattering as the asymptotic decay of the standing waves depends only upon τ_1 . However, Bürgi *et al.*¹¹ have misidentified the correct dependence of the standing wave patterns on the phase coherence length, so that their are actually twice τ_1 .²² The lifetimes determined by Braun and Rieder⁵ shown in Fig. 4 (∇) have been obtained from a detailed analysis of standing wave patterns in triangular corrals constructed from

Ag adatoms. In their analysis the Ag adatoms are not treated as “black-dot” scatterers, but as point scatterers whose scattering properties are determined by fitting, along with a phase coherence length which enters an attenuation factor $\exp -r/\tilde{L}_\Phi$ in the electron propagation between scattering events, and to and from the STM tip position. Thus lossy scattering effects are fully accounted for in this work – in so far as the two-dimensional point-scatterer model is valid – but again an incorrect relationship is used between the phase coherence length \tilde{L}_Φ and the lifetime τ_1 , leading to values that are twice τ_1 . Correcting for this, the agreement between the lifetimes found by Braun and Rieder and theoretical values for Ag(111), which are generally lower than those found in Ref. 5, is improved.

In summary we have investigated the lifetimes of electrons confined to vacancy islands with areas $\approx 40 - 220 \text{ nm}^2$ on Ag(111). We find that the geometry of the vacancy has only a weak influence on the lifetimes, which are dominated by lossy scattering at the steps which form the edges of the island. The lifetimes are well described by a theory that includes the dependence on the electron energy, vacancy size, step reflectivity and the phase coherence length. This indicates that the crossover to lifetimes dominated by electron-electron and electron-phonon scattering will occur for islands with dimensions an order of magnitude greater than those studied here. This result and a corrected analysis of published experimental data lead to a more consistent picture of surface state lifetimes in experiments and calculation.

H. J., J. K., and R. B. thank the Deutsche Forschungsgemeinschaft for financial support. S. C. acknowledges the support of the British Council.

* Electronic address: kroeger@physik.uni-kiel.de

† Electronic address: s.crampin@bath.ac.uk

¹ M. F. Crommie, C. P. Lutz, and D. M. Eigler, *Science* **262**, 218 (1993).

² E. J. Heller, M. F. Crommie, C. P. Lutz, and D. M. Eigler, *Nature (London)* **369**, 464 (1994).

³ J. Kliewer, S. Crampin, and R. Berndt, *Phys. Rev. Lett.* **85**, 4936 (2000).

⁴ J. Kliewer, S. Crampin, and R. Berndt, *New J. Phys.* **3**, 22 (2001).

⁵ K.-F. Braun and K.-H. Rieder, *Phys. Rev. Lett.* **88**, 096801 (2002).

⁶ J. Li, W.-D. Schneider, R. Berndt, and S. Crampin, *Phys. Rev. Lett.* **80**, 3332 (1998).

⁷ L. Bürgi, O. Jeandupeux, A. Hirstein, H. Brune, and K. Kern, *Phys. Rev. Lett.* **81**, 5370 (1998).

⁸ J. Li, W.-D. Schneider, S. Crampin, and R. Berndt, *Surf. Sci.* **422**, 95 (1999).

⁹ I. Barke and H. Hövel, *Phys. Rev. Lett.* **90**, 166801 (2003).

¹⁰ J. Kliewer, R. Berndt, E. V. Chulkov, V. M. Silkin, P. M. Echenique and S. Crampin, *Science* **288**, 1399 (2000).

¹¹ L. Bürgi, O. Jeandupeux, H. Brune, and K. Kern, *Phys. Rev. Lett.* **82**, 4516 (1999).

¹² L. Vitali, P. Wahl, M. A. Schneider, K. Kern, V. M. Silkin,

E. V. Chulkov, and P. M. Echenique, *Surf. Sci.* **523**, L47 (2003).

¹³ K. Morgenstern, G. Rosenfeld, B. Poelsema, and G. Comsa, *Phys. Rev. Lett.* **74**, 2058 (1995).

¹⁴ J. Li, R. Berndt, and W.-D. Schneider, *Phys. Rev. B* **56**, 7656 (1997).

¹⁵ S. Crampin, M. H. Boon, and J. E. Inglesfield, *Phys. Rev. Lett.* **73**, 1015 (1994).

¹⁶ S. Crampin and O. R. Bryant, *Phys. Rev. B* **54**, R17367 (1996).

¹⁷ S. Crampin, M. Nekovee, and J. E. Inglesfield, *Phys. Rev. B* **51**, 7318 (1995).

¹⁸ S. Crampin, J. Kröger, H. Jensen, and R. Berndt, unpublished.

¹⁹ P. M. Echenique and J. B. Pendry, *J. Phys. C: Solid State Phys.* **11**, 2065 (1978).

²⁰ N. V. Smith, *Phys. Rev. B* **32**, 3549 (1985).

²¹ A. Eiguren, B. Hellsing, F. Reinert, G. Nicolay, E. V. Chulkov, V. M. Silkin, S. Hüfner, and P. M. Echenique, *Phys. Rev. Lett.* **88**, 066805 (2002).

²² S. Crampin, J. Kröger, H. Jensen, and R. Berndt, *cond-mat/0410542*.